Sex-specific co-expression networks and sex-biased gene expression in the salmonid Brook Charr *Salvelinus fontinalis*

Ben J. G. Sutherland[1†*], Jenni M. Prokkola[2], Céline Audet[3], and Louis Bernatchez[1]

[1] Institut de Biologie Intégrative et des Systèmes (IBIS), Université Laval, Québec, QC G1V 0A6, Canada

[2] Institute of Integrative Biology, University of Liverpool, L69 7ZB Liverpool, UK

[3] Institut des Sciences de la Mer de Rimouski, Université du Québec à Rimouski, Rimouski, QC G5L 3A1, Canada

[†]Current Address: Pacific Biological Station, Fisheries and Oceans Canada, Nanaimo, BC, V9T 6N7, Canada

*Author for correspondence: BJGS
Pacific Biological Station, Fisheries and Oceans Canada, Nanaimo, BC, Canada
Phone: 1 (250) 751-4676
Email: ben.sutherland.1@ulaval.ca (BS)

Data Deposition: Brook Charr raw sequence data has been uploaded to SRA under BioProject PRJNA445826, accession SRP136537. Arctic Charr raw sequence data is available under BioProject PRJNA307980, accession SRP068854.

ABSTRACT

Networks of co-expressed genes produce complex phenotypes associated with functional novelty. Sex differences in gene expression levels or in the structure of gene co-expression networks can cause sexual dimorphism and may resolve sexually antagonistic selection. Here we used RNA-sequencing in the paleopolyploid salmonid Brook Charr *Salvelinus fontinalis* to characterize sex-specific co-expression networks in the liver of 35 female and 51 male offspring. In both networks, modules were characterized for functional enrichment, hub gene identification, and associations with 15 growth, reproduction, and stress-related phenotypes. Modules were then evaluated for preservation in the opposite sex, and in the congener Arctic Charr *Salvelinus alpinus*. Overall, more transcripts were assigned to a module in the female network than in the male network, which coincided with higher inter-individual gene expression and phenotype variation in the females. Most modules were preserved between sexes and species, including those involved in conserved cellular processes (e.g. translation, immune pathways). However, two sex-specific male modules were identified, and these may contribute to sexual dimorphism. To compare with the network analysis, differentially expressed transcripts were identified between the sexes, finding a total of 16% of expressed transcripts as sex-biased. For both sexes, there was no overrepresentation of sex-biased genes or sex-specific modules on the putative sex chromosome. Sex-biased transcripts were also not overrepresented in sex-specific modules, and in fact highly male-biased transcripts were enriched in preserved modules. Comparative network analysis and differential expression analyses identified different aspects of sex differences in gene expression, and both provided new insights on the genes underlying sexual dimorphism in the salmonid Brook Charr.

Keywords: Co-expression; Salmonid; Sex-bias; Sexual Dimorphism; Transcriptomics; Weighted Gene Co-expression Network Analysis (WGCNA)

INTRODUCTION

Understanding how sex bias in gene expression contributes to sexually dimorphic phenotypes, and how this affects fitness is an important area of study to understand genotype-phenotype interactions (Parsch and Ellegren 2013). The development of sex differences in phenotypes can be attributed to differences in the expression of both sex-specific and autosomal genes, caused by hormonal and epigenetic effects (Ellegren and Parsch 2007; Wijchers and Festenstein 2011), heterogamy and imperfect dosage compensation (Parsch and Ellegren 2013), epistatic interactions, and transcriptional network structural differences (Chen *et al.* 2016). Sex-biased gene expression is pervasive in many species and may alleviate sexually antagonistic selection, i.e., the selection for different phenotypes in the different sexes (Wright *et al.* 2018; Rowe *et al.* 2018). Transcriptome regulatory architecture differences between the sexes may contribute to the development of sex-biased gene expression (Chen *et al.* 2016; Wright *et al.* 2018). Sex-biased expression underlies much of phenotypic sexual dimorphism, which can occur without sexually antagonistic selection (e.g. imperfect dosage compensation; Parsch and Ellegren 2013). To connect alleles to phenotypes, typically association studies are applied (Mackay, 2001; Bush and Moore 2012), but these bypass important intermediate regulatory steps such as transcriptome regulation (Mackay *et al.* 2009) . To characterize transcriptome regulation, it is important to consider the underlying structure of the network in which genes are co-regulated (Mähler *et al.* 2017).

Constructing gene co-expression networks is often based on correlating transcript abundance across samples (Langfelder and Horvath 2008). A network is comprised of modules, each of which is comprised of a group of genes with correlated expression patterns. Co-expression clustering is a valuable approach to classify and visualize transcriptomic data (Eisen *et al.* 1998). Clustering often groups genes together that have similar cellular functions and regulatory pathways (Eisen *et al.* 1998), although this is not always the case (Gillis and Pavlidis 2012; van Dam *et al.* 2017). Module functions can be predicted based on phenotypic correlations (Filteau *et al.* 2013; Rose *et al.* 2015) or functional enrichment analysis (e.g. Gene Ontology). Genes that are highly connected and central to a module (i.e., hub genes) may be upstream regulators of the module, and potentially more related to the module function (van Dam *et al.* 2017). Hub genes may also be under higher selective constraint than other less connected genes, and as a result may show lower genetic variation and higher phylogenetic conservation (Mähler *et al.* 2017). Network information thus provides novel insight into both gene activity and evolution.

Comparative network analysis across species can advance the understanding of species-specific innovations. For example, comparing brain transcriptome networks between chimpanzee *Pan troglodytes* and human *Homo sapiens* indicates low preservation of modules found in specific brain regions associated with human evolution such as the cerebral cortex (Oldham *et al.* 2006). Comparing networks can highlight potential drivers of phenotypic changes associated with adaptive divergence that can lead to

ecological speciation (Filteau *et al.* 2013; Thompson *et al.* 2015). Cross-species network comparisons have also been used to detect gene modules associated with disease (Mueller *et al.* 2017) or with seasonal phenotypic changes (Cheviron and Swanson 2017). These insights are often not possible to obtain through standard gene-by-gene differential expression analysis, which captures a smaller proportion of the variation than differential co-expression analysis (Oldham *et al.* 2006; Gaiteri *et al.* 2014).

Network comparisons can also provide insight on sex differences (Chen *et al.* 2016). Differing structure of networks between the sexes may resolve sexual antagonism through gene regulation (Chen *et al.* 2016). Other genetic architecture solutions to this conflict may include sex-dependent dominance (Barson *et al.* 2015) or maintaining alleles associated with sexual antagonism on sex chromosomes (Blackmon and Brandvain 2017). Comparisons between the sexes are complicated by the fact that sex bias in networks can be tissue-specific, with modules more preserved between sexes in brain and muscle networks than in liver or adipose tissue (van Nas *et al.* 2009; Wong *et al.* 2014). Liver tissue is considered a highly sexually dimorphic tissue, particularly in oviparous species at a reproductive stage (Qiao *et al.* 2016). Although the extent of differences may depend on the tissue of study, network comparisons between sexes can provide new insight into the regulatory underpinnings of sexual dimorphism and antagonism.

Salmonids are an important species of commercial, ecological, and cultural value. This species group is also a model system for studying genome evolution after a whole genome duplication event that occurred approx. 60-88 million years ago (Allendorf and Thorgaard 1984; Crête-Lafrenière *et al.* 2012; Macqueen and Johnston 2014). Charr (*Salvelinus* spp.) are a phenotypically diverse group within Family Salmonidae that are less characterized in terms of transcriptomic and genomic data than other genera (e.g. *Salmo* or *Oncorhynchus*; but see Christensen *et al*. 2018). Brook Charr *Salvelinus fontinalis* is a primarily freshwater species native to Eastern North America. Arctic Charr *S. alpinus* has a circumpolar distribution mainly in the Arctic, and these two lineages diverged approximately 10 million years ago (Horreo 2017). Sexual dimorphism in body size, for example, is associated with reproductive success in Brook Charr. The largest males are typically dominant and fertilize the majority of a brood (Blanchfield *et al.* 2003). However, smaller sneaker males can also contribute in this same fertilization, albeit to a lesser extent than the large male. In females however, large body size is more constrained as it is highly associated to fecundity, and smaller life history variants are not expected (reviewed by Fleming 1998). In other salmonids, body size and secondary sexual characteristics (e.g. dorsal hump size) are also favoured male traits (Quinn and Foote 1994). With different optimal reproductive-associated phenotypes between the sexes, this could give rise to sexual dimorphism as well as sexual antagonism.

Here we profile liver transcriptomes of 100 Brook Charr offspring from a single family by RNA-sequencing to characterize co-expression patterns. Transcriptome profiling was conducted shortly (3 h)

after the application of an acute handling stressor to all individuals during the reproductive season, increasing variance among individuals. The goals of this study are to i) characterize the sex-specific or preserved modular structure of gene co-expression in liver tissue in Brook Charr; ii) characterize module preservation in the congener Arctic Charr; iii) connect phenotype and functional category associations to the identified modules; and iv) integrate results from the network analyses with a gene-by-gene differential expression analysis to determine whether the two methods provide different insights on sexual dimorphism in transcriptome architecture.

METHODS

Animals and sample collection

Brook Charr used in this study were originally used to construct a low-density genetic map for reproductive (Sauvage, Vagner, Derôme, Audet, and Bernatchez 2012a), growth and stress response QTL analyses (Sauvage, Vagner, Derôme, Audet, and Bernatchez 2012b). They were used to construct a high-density genetic map that was integrated with the other salmonids (Sutherland *et al.* 2016), then used to identify QTL, sex-specific recombination rates, and the Brook Charr sex chromosome (Sutherland *et al.* 2017). The 192 F_2 individuals were full sibs from a single family resulting from a cross of an F_1 female and F_1 male that were from an F_0 female from a wild anadromous population (Laval River, near Forestville, Québec) and an F_0 male from a domestic population (Québec aquaculture over 100 years).

F_2 offspring were raised until 65-80 g and then 21 phenotypes were collected along with several repeat measurements to determine growth rate. Full details on these phenotypes are previously described (Sauvage *et al.* 2012a, 2012b), including sex-specific phenotype averages, standard deviations, and phenotype correlations for all 192 offspring (see Table S1 and Figure S2 from Sutherland et al. 2017). The 15 phenotypes used in the present study to correlate with co-expression modules were maturity, length, weight, growth rate, condition factor, liver weight, post-stress cortisol, osmolality and chloride, change in cortisol, osmolality and chloride between one week before and three hours after an acute handling stress, egg diameter, sperm concentration, and sperm diameter. Fish were anaesthetized with 3-aminobenzoic acid ethyl ester and killed by decapitation as per regulations of Canadian Council of Animal Protection recommendations approved by the University Animal Care Committee, as previously reported (Sauvage *et al.* 2012a). Most individuals were in a reproductive state at the time of the dissection, which was in the fall (smolting occurs in this strain in the spring; Boula *et al.* 2002). Phenotypic sex was determined by gonad inspection (Sauvage *et al.* 2012b). Immediately after decapitation, liver tissue was excised, flash frozen then kept at -80 ^{o}C until RNA extraction.

152 *RNA extraction and library preparation*

153 A total of 100 of the 192 individuals were used for liver transcriptome profiling. Prior to extraction,
154 samples were assigned random order to reduce batch effects on any specific group of samples. Total RNA
155 was extracted from equal sized pieces of liver tissue from approximately the same location on the liver for
156 all samples (0.4 x 0.2 x 0.2 cm; ~1 mg). This piece was rapidly immersed in 1 ml TRIzol (Invitrogen),
157 then placed on dry ice until all samples per batch were prepared (6-12 per extraction round). When all
158 samples were ready, the samples immersed in frozen TRIzol were allowed to slightly thaw for
159 approximately 1 min until beads within the vials were able to move, then the samples were homogenized
160 for 3 min at 20 hz, rotated 180°, and homogenized again for 3 min at 20 hz on a MixerMill (Retsch). The
161 homogenate was centrifuged at 12,000 x g for 10 min at 4 ^{o}C. The supernatant was transferred to a new 2
162 ml tube and incubated for 5 min at room temperature. Chloroform (200 µl) was added to the tube, the tube
163 was shaken vigorously for 15 s and incubated 3 min at room temperature, then centrifuged at 12,000 x g
164 for 15 min at 4 ^{o}C. Finally the aqueous layer was carefully transferred to a new centrifuge tube, and into
165 an RNeasy spin column (QIAGEN), as per manufacturer's instructions with the optional on-column
166 DNase treatment. All samples were quality checked using a BioAnalyzer (Agilent), where all samples had
167 RIN ≥ 8.3 (mean = 9.5), and were quantified using spectrophotometry on a Nanodrop-2000 (Thermo
168 Scientific).

169 Libraries were prepared using 1 µg of total RNA in the randomized order using TruSeq RNA
170 Sample Prep Kit v2 (Illumina) to generate cDNA as per manufacturer's instructions using adapters from
171 both Box A and Box B, AMPure XP beads (Agencourt) and a magnetic plate in batches of 8-16 samples
172 per batch. Fragmentation times of 2, 4 and 6 min were tested for optimal size fragmentation and
173 consistency, and as a result of this test, all samples were processed using a 6 min fragmentation time.
174 PCR amplification to enrich cDNA was performed using 15 cycles, as per manufacturer's instructions.
175 All libraries were quantified using Quant-iT PicoGreen (ThermoFisher) and quality-checked using the
176 BioAnalyzer on High Sensitivity chips (Agilent). Once all samples were confirmed to be high quality and
177 of approximately the same insert size, eight individually tagged samples were pooled in equimolar
178 quantities (80 ng per sample) and sent to McGill Sequencing Center for 100 bp single-end sequencing on
179 a HiSeq2000 (Illumina; total = 13 lanes). Parents (F_1 individuals) were sequenced in duplicate in two
180 separate lanes.

181

182 *RNA-seq mapping*

183 Quality trimming and adapter removal was performed using Trimmomatic (Bolger et al. 2014), removing
184 adapters with the *-illuminaclip* (2:30:10) option and removing low quality reads (< Q2) using -
185 *slidingwindow* (20:2), *-leading* and *-trailing* options. Q2 was used for optimal quantification as previously

186 demonstrated (MacManes 2014). A reference transcriptome for Brook Charr was obtained from the
187 Phylofish database (Pasquier *et al.* 2016). Trimmed reads were mapped against the reference
188 transcriptome with *bowtie2* (Langmead and Salzberg 2012) using *--end-to-end* mode reporting multiple
189 alignments (*-k* 40) for optimal use with eXpress for read count generation (Roberts and Pachter 2013).
190 The multiple alignment file was converted to bam format and sorted by read name using SAMtools (Li *et*
191 *al.* 2009) and input to eXpress (see full bioinformatics pipeline in *Data Accessibility*).
192 Read counts were imported into edgeR (Robinson et al. 2010) for normalization and low
193 expression filtering. The smallest library (lib87, 8,373,387 aligned reads) was used to calculate a low-
194 expression threshold. A count-per-million threshold of 10 reads per transcript in this library defined the
195 threshold for transcript retention (cpm > 1.19), as suggested in the edgeR documentation. Any transcript
196 passing this threshold in at least five individuals was retained through the first filtering step for initial data
197 visualization and annotation. Additional low expression filtering was conducted in the differential
198 expression analysis and network analysis (see below). Although transcripts were previously annotated in
199 the Phylofish database (Pasquier *et al.* 2016), each transcript was re-annotated using trinotate (Bryant *et*
200 *al.* 2017) and *tblastx* against Swissprot (cutoff = $1e^{-5}$) to obtain as many identifiers as possible for Gene
201 Ontology enrichment analysis. For individual gene descriptions, the re-annotated Swissprot identifier was
202 used primarily, and the Phylofish annotation secondarily.
203
204 *Differential expression analysis between sexes*
205 To reduce the number of transcripts with very low expression in the differential expression analysis, we
206 applied a low expression filter of cpm > 1.19 in at least 65% of the individuals from each sex (i.e. ≥ 31 /
207 47 females or 35 / 53 males). The data was then normalized using the weighted trimmed mean of M-
208 values (TMM Robinson and Oshlack 2010) to generate normalized $\log_2$ expression levels. Using
209 *model.matrix* from edgeR with sex as the data grouping, a genewise negative binomial generalized linear
210 model (*glmFit*) was fit to each gene. Genes with false discovery rate of ≤ 0.05 and linear fold-change ≥
211 1.5 were defined as differentially expressed. These genes were binned into low sex bias (i.e. 1.5 ≤ FC ≤ 4)
212 or high sex bias (i.e. FC > 4) for each sex (negative FC for females, positive for males), as per previous
213 delimitations (Poley *et al.* 2016).
214
215 *Weighted gene co-expression network analysis (WGCNA) in Brook Charr*
216 To best associate modules with phenotypes of interest, sexes were analyzed separately, with preservation
217 evaluated in the opposite sex (Langfelder *et al.* 2011). Due to the independent analysis of each sex, low
218 expression filters (i.e. cpm > 0.5 in at least five individuals) were conducted separately in each sex, then
219 the data normalized as described above. The average library size was 27,896,535 alignments, indicating

220 cpm > 0.5 corresponds to at least 13.95 reads aligning to the transcript for this mean library size. Sex-
221 specific data was used as an input for weighted gene correlation network analysis (WGCNA; Langfelder
222 and Horvath 2008; 2012) in R (R Core Team 2018).

223 Within each sex, sample outliers were detected and removed by clustering samples based on
224 transcript expression by Euclidean distance and visually inspecting relationships with the *hclust* average
225 agglomeration method of WGCNA (Langfelder and Horvath 2008). Removal of outliers prevents
226 spurious correlations of modules due to outlier values and improves network generation (Langfelder *et al.*
227 2011). Remaining samples were then correlated with trait data using *plotDendroAndColors*. Network
228 parameters for both female and male networks were defined as per tutorials using unsigned correlation
229 networks (Langfelder and Horvath 2008). Unsigned networks consider the connectivity between identical
230 positive or negative correlations to be equal, and thus genes in the same module may have similar or
231 inverse expression patterns. An optimal soft threshold power (6) was identified by evaluating effects on
232 the scale free topology model fit and mean connectivity by increasing the threshold power by 1 between
233 1-10 and by 2 between 12-20 (Figure S1), as suggested by Langfelder and Horvath (2008). An unsigned
234 adjacency matrix was generated in WGCNA to identify the 25,000 most connected transcripts to retain
235 for reducing computational load. Then, to further minimize noise and spurious associations, adjacency
236 relationships were transformed to the Topological Overlap Matrix using the *TOMdist* function
237 (Langfelder and Horvath 2008).

238 Similarity between modules was evaluated using module eigengenes (i.e. the first principal
239 component of the module). Dissimilarity between eigengenes was calculated by signed Pearson
240 correlation as suggested by Langfelder and Horvath (2008) and plotted using *hclust.* When modules were
241 more than 0.75 correlated (dissimilarity 0.25), they were merged as suggested by Langfelder and Horvath
242 (2008). Merged module eigengenes were then tested for associations with phenotypes by Pearson
243 correlation. Notably the sign of the correlation does not necessarily indicate the direction of the
244 relationship between the expression of specific genes in each module and the phenotype because the
245 modules were built using unsigned networks.

246 Module membership (i.e., the module eigengene-gene correlation) was used to define the top
247 central transcripts for each module (i.e., hub genes). Gene significance (i.e., the absolute value of the trait-
248 gene correlation) was calculated for each transcript against traits weight, specific growth rate, condition
249 factor, hepatosomatic index, change in cortisol, osmolality and chloride from the brief handling stressor,
250 female egg diameter, and male sperm concentration and diameter. Module eigengenes were tested for
251 correlation against traits using Pearson correlation ($p \leq 0.01$).

252 Gene Ontology enrichment analysis of transcripts within each module was conducted using the
253 re-annotated Swissprot identifiers in DAVID Bioinformatics (Huang *et al.* 2009). Heatmaps for modules

254 of interest were generated by using the package *gplots* using the normalized $\log_2$ cpm data (Warnes *et al.*
255 2016). Expression values were standardized across samples for each transcript and Pearson correlation
256 was used to cluster transcripts and samples.

257 To determine sex-specific or sex-conserved modules, module preservation was evaluated by
258 comparing male transcript expression to the generated female modules, and visa-versa, using the
259 *modulePreservation* function of WGCNA. A total of 200 permutations of randomly assigned module
260 labels were used to calculate module preservation rank and Zsummary (Langfelder *et al.* 2011). Low
261 Zsummary scores indicate no preservation (≤ 2), intermediate indicate moderate preservation (2-10) and
262 high scores (≥ 10) indicate strong module preservation (Langfelder *et al.* 2011). Module quality was also
263 determined for each module as a measure of module robustness that is characterized by conducting the
264 analysis on multiple random subsets of the original data (Langfelder *et al.* 2011). In addition, cross-
265 tabulation of the proportions of female modules in male modules and visa-versa were performed in R.
266 Cross-tabulation requires similar modular structures of the compared networks, whereas adjacency
267 comparisons directly compare co-expression independent of network topology. All pipelines to analyze
268 the current data are documented and available on GitHub (see *Data Accessibility*).
269

270 *Module preservation in Arctic Charr*

271 To compare module preservation between Brook Charr and Arctic Charr *S. alpinus* we used RNA-seq
272 data from 1+ year-old Arctic Charr. The broodstock of this population was reared in hatchery conditions
273 for three generations after being collected from a subarctic, land-locked population in Finland (Lake
274 Kuolimo, 61°16′ N; 27°32′ E). The data were collected from nine male liver samples (fish relatedness not
275 known) from each of 8 ^{o}C and 15 ^{o}C (total = 18 samples), but due to a large effect of temperature on the
276 transcriptome, and differences between sampling times in the 15 ^{o}C group, only the nine samples from the
277 8 ^{o}C, group were used here (normal rearing temperature during summer at the fish hatchery; Figure S2)
278 (Prokkola *et al.* 2018). Fish body mass at 8°C was on average 24.2 g ± standard deviation (S.D.) 10.4 g.

279 Sample processing was explained fully by Prokkola et al (2018) and briefly described here. In
280 August 2013, fish were euthanized using 200 ppm sodium bicarbonate-buffered tricaine methanesulfonate
281 (MS-222), after which liver samples were collected and flash frozen in liquid nitrogen (Prokkola *et al*.
282 2018). RNA was extracted from approximately 10 mg of liver tissue using Tri-reagent (Molecular
283 Research Center), and quality checked using a BioAnalyzer (Agilent), with an average identified RNA
284 integrity number of 9.95. Strand-specific cDNA library preparation and sequencing were conducted at
285 Beijing Genomics Institute (BGI Hong Kong) using TruSeq RNA Sample Prep Kit v2 (illumina) and
286 sequenced on an Illumina HiSeq2000 instrument to generate paired-end 100 bp reads. All samples were
287 pooled with unique barcodes across four sequencing lanes. Adapters were removed at BGI, and reads

288 trimmed with Trimmomatic (Bolger et al. 2014) using options *leading* and *trailing* (5) *slidingwindow*
289 (4:15) and *minlen* (36). From samples included in this study, on average 41.7 ± S.D. 7.4 million reads
290 were obtained.

291 Transcript expression was calculated as above, including using the Brook Charr reference
292 transcriptome for ease of cross-species comparisons. Low expression filtering and normalization for the
293 Arctic Charr data was conducted as above (cpm > 0.5 in at least five individuals). However, a network
294 was not constructed for these samples. Using samples from both temperatures, modules were previously
295 identified (Prokkola *et al.* 2018). Once normalized and input to WGCNA, read counts in Arctic Charr 8°C
296 samples were used to build a gene adjacency matrix, which was then compared against modules generated
297 for female and male Brook Charr samples using the *modulePreservation* function as described above.
298 Caveats regarding this data should be noted, including the smaller sample size, immature state of Arctic
299 Charr, minor differences in rearing environments (albeit both were reared in hatchery conditions), and
300 unknown relatedness.

301

302 *Identifying one transcript per gene and assigning chromosome positions*

303 The Brook Charr reference transcriptome (Pasquier *et al.* 2016) possibly contains multiple isoforms for a
304 single gene (Y. Guiguen, *pers. comm.*). Therefore an approach was taken here to reduce multiple genes to
305 a single transcript per gene for enrichment analyses on the sex chromosome or in sex-specific modules.
306 First, the Brook Charr reference transcriptome was aligned to the Atlantic salmon *Salmo salar*
307 chromosome-level genome assembly RefSeq GCF_000233375.1 (Lien *et al.* 2016) using GMAP (Wu and
308 Watanabe 2005). Alignments were converted to an indexed bam retaining only high quality (-q 30)
309 alignments using samtools (Li *et al.* 2009). The indexed bam was converted to a bed file using bedtools
310 *bamtobed* (Quinlan and Hall 2010). Second, the lengths of Brook Charr transcripts were calculated using
311 custom python scripts (see *Data Accessibility*). With the alignment position, lengths, and expression
312 status (expressed or not expressed), a single transcript per contiguous (or overlapping) alignment block on
313 the reference genome was retained using a custom R script (see *Data Accessibility*). For each contiguous
314 alignment block, this script preferentially retained the longest, expressed transcript. All other redundant
315 transcripts, and all that did not align, were not retained. In some cases, a single transcript can align to
316 multiple locations with high mapping quality (MAPQ ≥ 30). Since there was no reason to retain one
317 alignment over another, both alignments were retained in the baseline set for these cases.

318 The alignment information per retained Brook Charr transcript was used to assign an Atlantic
319 Salmon chromosome identifier to each retained unique transcript. The chromosome information was
320 combined with the module information for all transcripts in each sex-specific network. This analysis was
321 conducted separately for females and males, as expressed genes were in some cases different between the

322 two sexes and therefore so would be the selection of which transcript to retain. The correspondence
323 between the Atlantic Salmon genome assembly accession identifier and the Atlantic Salmon chromosome
324 identifier were obtained from the NCBI genome assembly website (see *Data Accessibility*). In general,
325 correspondence of gene synteny is expected to be similar between Atlantic Salmon and Brook Charr
326 (Sutherland *et al.* 2016). Using the chromosome correspondence table in Sutherland et al. (2016), the
327 Atlantic Salmon chromosome containing the sex chromosome of Brook Charr was identified. For each
328 sex-specific co-expression module, the proportions of Brook Charr genes located on the Atlantic Salmon
329 chromosome that corresponds to the Brook Charr sex chromosome were characterized and compared to
330 the total list of all non-redundant Brook Charr transcripts identified. Fisher exact tests were then used to
331 determine significance for each sex-specific module-sex chromosome combination (i.e., two tests). The
332 chromosome information was also combined with the sex bias fold change values. Finally, the proportion
333 of highly or moderately sex-biased transcripts for females and males were investigated for
334 overrepresentation on the sex chromosome and in sex-specific or conserved modules using Fisher's exact
335 tests in custom R scripts (see *Data Availability*).
336

337 # RESULTS

338 *Transcriptome overview*

339 Of the total 69,440 transcripts in the Brook Charr reference transcriptome, 51,911 passed initial low
340 expression filters when using all samples together. Low-expression filtering for differential expression
341 analysis (i.e., expressed in at least 65% of individuals from one of two sexes) resulted in the retention of
342 42,622 transcripts. Low-expression filtering for sex-specific network analysis (i.e., expressed in at least
343 five individuals of the sex of interest) resulted in 50,748 and 50,530 transcripts passing filters in females
344 and males, respectively. When considering each sex individually, most of the expressed genes were
345 expressed in a majority of the samples: females expressed 35,461 transcripts in > 90% of the samples;
346 males expressing 35,714 transcripts in > 90% of the samples (Figure S3).

347 Hierarchical clustering of samples by gene expression indicated a large effect of sex, where 35 of
348 47 F_2 females clustered with the F_1 female, and 52 of 53 F_2 males were clustered together with the F_1 male
349 (Figure 1). As described in the Methods, outliers were removed to avoid spurious network correlations
350 (Langfelder *et al.* 2011), and this included the removal of one male leaving 52 males remaining, and the
351 removal of one group of females that had large liver weight, leaving 35 females remaining (see phenotype
352 liver weight in Figure 1; Figure S4). When these outlier samples were included while constructing the
353 female network, many modules correlated with the liver weight phenotype, suggesting that these samples
354 were having a large impact on the network.

Interestingly, females displayed higher inter-individual variance than males, as indicated by the multiple smaller sample clusters of females in the hierarchical clustering relative to the fewer and larger sample clusters of the males (Figure 1). Likewise, six of the phenotypic traits also displayed higher variance in females (significant heteroscedasticity at $P < 0.05$, Levene's test): liver weight, cortisol level, osmolality, and change in cortisol, osmolality and chloride levels due to handling (Figure S5). Some of the higher variance in these traits in females was likely explained by maturity, but maturity did not explain all of the variance within the female gene expression, as the different sample clusters observed had a variety of maturity states, and samples that were all considered mature were present in different sample clusters (Figure 1).

Network construction and phenotype correlations: female Brook Charr

Highly correlated module eigengenes ($r > 0.75$) were merged, combining 81 assigned modules into 14 (Figure S6A; Figure S7A). Assigned female modules each contained a range of 77-10,533 transcripts (Table 1). The largest module was *darkred*, with 10,533 transcripts (see Table 1), which included more transcripts than even the unassigned *grey* module (second largest; 5,892 transcripts).

Phenotype ($n = 15$) correlations with module eigengenes indicate potential functional associations of the modules (Table 1; Figure 2). The strongest associations of phenotypes to modules were with maturity index, for example with *thistle2* ($r > 0.81$), and *coral1* ($r = -0.83$). Although the large liver weight outlier samples were removed prior to network generation, liver weight remained highly correlated with *indianred4* ($r = 0.73$), *salmon*, *coral* ($r = 0.52$), and *blue2* ($r = -0.64$). Growth rate showed similar module correlations to liver weight (Figure 2). Osmolality change was also correlated with *indianred4* ($r = 0.56$) and *blue2* ($r = -0.58$), as well as with *darkred*, *thistle3* ($r \geq 0.51$), *darkorange*, *green* and *darkmagenta* ($r \geq |-0.49|$). Chloride change had no significant associations, but post-stress chloride was correlated with *thistle3* ($r = 0.56$) and *lightsteelblue* ($r = -0.53$). Although no modules were significantly associated with cortisol (change or post-stress; $p \geq 0.01$), *ivory* was close ($r = -0.38$; $p = 0.03$).

In order to understand the gene composition of modules, Gene Ontology functional enrichment analysis of the transcripts within each module was conducted (Table 1; Additional File S1). The *salmon* module (correlated with liver weight) was enriched for erythrocyte development. The *blue2* module (liver weight) was associated with ribonucleoprotein complex. *Darkorange*, *green*, and *darkmagenta* modules (all correlated with osmolality change) were enriched for small molecular metabolic process, translation and metabolism functions, respectively. One module did not have significant enrichment of biological processes, *lightsteelblue* (correlated with chloride change).

Preservation of co-expression: female Brook Charr network

The preservation of co-expression of female Brook Charr modules in Brook Charr males was primarily evaluated using network adjacency comparisons, which are more sensitive and robust than cross-tabulation methods (Langfelder *et al.* 2011). Most female modules were preserved in males and only *darkred* had weak evidence for preservation (Table 1). *Green* was the most conserved (Zsummary = 100), followed by *blue2*, *salmon*, *lightsteelblue* and *darkorange* (Zsummary ≥ 48; Table 1). Modules associated with translation activities were among the highest conserved modules (e.g. *green* and *blue2*).

Published male Arctic Charr liver transcriptome data was then compared to the network to evaluate cross-species module preservation (Prokkola *et al.* 2018). Even with caveats regarding sample size (see Methods), several female Brook Charr modules were highly preserved in Arctic Charr males, including *blue2* (Zsummary = 34), *green* (Zsummary = 24), and *salmon* (Zsummary = 17), also the most conserved in male Brook Charr (Table 1). Other female Brook Charr modules with moderate evidence for preservation in male Arctic Charr included *darkorange* and *lightsteelblue* (Zsummary > 8), which were also highly preserved in male Brook Charr. It is noteworthy that the ranking of preservation of female modules in the Arctic Charr and Brook Charr males is highly similar (Table 1).

Network construction, phenotype correlations, and sex-specificity: male Brook Charr

Highly correlated male modules (eigengene correlation r > 0.75) were merged, reducing 44 assigned male modules to 25 (Figure S6B; Figure S7B). Unlike the female network, a large proportion of the male data could not be assigned to a module. The unassigned *grey* module contained 72% of the analyzed transcripts (17,992 transcripts). Assigned modules each contained between 54-1,732 transcripts (Table 2; Additional File S2). Phenotypic correlations with male module eigengenes were tested (Figure S8; see Supplemental Results; summarized in Table 2). Of note were several modules enriched for immunity-related functions, including *darkmagenta* (defense response to virus) and *steelblue* (positive regulation of innate immune response) (Table 2 and Additional File S1). These two immune processes were found to belong to different modules that were not just inversely regulated (in an unsigned network such as this, these would be grouped), but likely having decoupled regulation (Figure 3A), although the modules were still correlated (Figure S7B).

Preservation of male modules in females was also evaluated, but in contrast to what was observed in the preservation of female modules in males (see above), many of the male modules were weakly to moderately preserved in the females. Highly preserved modules included *yellow* (Zsummary = 58; Figure 3B) and *brown* (Zsummary = 38), *tan* (Zsummary = 43), and *lightcyan* (Zsummary = 34). Some modules were less preserved than even the randomly generated *gold* module (Table 2) and the unassigned *grey* module, including *green* (translation and size; Zsummary = 4.5), *darkgrey* (mitochondrial membrane;

422 Zsummary = 1.8) and *ivory* (transcription factor activity; Zsummary = 0.8; Figure 3C), suggesting the co-
423 expression trends in these modules are less preserved between the sexes. Preserved modules *yellow* and
424 *brown* were enriched for ribosomal or translation-related functions, as was the less preserved *green*
425 module (Table 2). *Ivory*, the most sex- and species-specific male module (see below; Table 2; Figure 3C)
426 was enriched for neurogenesis in GO biological process, but also transcription factor activity in GO
427 molecular function (Additional File S1). Other non-preserved or lowly preserved modules were enriched
428 for membrane activity including *darkgrey* (mitochondrial inner membrane) and *lightcyan1* (membrane
429 organization; Additional File S1). Preservation of male Brook Charr modules was also explored in Arctic
430 Charr males. Similar to that observed in the female modules, when a male Brook Charr module was
431 preserved in female Brook Charr, it was also often preserved in male Arctic Charr (see similar ranking of
432 preservation; Table 2).
433
434 *Sex-biased expression, sex-specific modules, and the sex chromosome*
435 Of the 42,622 expressed transcripts, 6,983 (16.4%) were differentially expressed (FC ≥ 1.5; glmFit FDR ≤
436 0.05). Female-biased genes included 3,989 moderately (1.5-4-fold) and 236 highly biased (>4-fold)
437 transcripts. Highly biased transcripts included known sex-biased genes such as *vitellogenin*, and *zona*
438 *pellucida sperm-binding proteins*. Male-biased genes included 2,638 moderately and 120 highly biased
439 transcripts, including *semaphorin-3F* (most highly male-biased transcript). For a complete list, see
440 Additional File S3.
441 Sex-biased transcripts were not overrepresented in female or male sex-specific modules (Table
442 3). However, unexpectedly, highly male-biased genes were overrepresented in highly preserved modules
443 (36 transcripts in highly preserved modules, 97% of the highly sex-biased transcripts) in comparison to
444 the overall percentage in the network (4,886 transcripts in highly preserved modules, 76.5% of network
445 transcripts; Table 3; two-sided Fisher's exact test p = 0.0013). The female data was more similar between
446 the highly sex-biased transcripts and the entire network (45.2% and 46.6%, respectively). Sex-specific
447 modules were not enriched on the sex chromosome (Fisher's exact test p > 0.5), including male modules
448 *ivory* and *darkgrey* (Table S1).
449 Of the 47 non-overlapping, highly male-biased transcripts assigned to chromosomes, five were on
450 the sex chromosome (10.6%), relative to 779 on the sex chromosome of the 12,934 expressed in males
451 (Ssa09; 6.0%). However, this difference was not significant (one-tailed Fisher's exact test p = 0.15).
452 Furthermore, moderately male-biased transcripts were not enriched on the sex chromosome (5.3%)
453 relative to all expressed transcripts (6%), nor were highly or moderately female-biased transcripts (high
454 bias = 4.1%; moderate bias = 5.8%).
455

456 # DISCUSSION

457 Gene co-expression produces complex phenotypes and may underlie key aspects of phenotypic evolution
458 (Filteau *et al.* 2013) and sexual dimorphism (Chen *et al.* 2016). One of the main challenges in producing
459 females and males is developing different phenotypes from largely the same set of genes (Rowe *et al.*
460 2018). Transcriptome architecture may provide a solution to this challenge. In this study, co-expression
461 networks for both female and male Brook Charr liver transcriptomes were characterized and compared to
462 each other. Although the female network had much higher module assignment of expressed transcripts, in
463 general most modules were preserved between the sexes. Two sex-specific modules were identified in
464 males that may provide insight on the evolution of gene expression and phenotypic sexual dimorphism.
465 Sex bias was observed in 16% of the expressed transcripts, and these sex-biased transcripts were not
466 overrepresented in sex-specific modules, indicating the different results obtained from these two analysis
467 approaches.
468
469 *Sex differences in co-expression networks and cross-species preservation*
470 Females and males clustered distinctly in unsupervised clustering by gene expression, as has been
471 observed in other studies of fish liver at a reproductive stage (Qiao *et al.* 2016). Interestingly, there was a
472 large difference in the number of transcripts assigned to modules between the sexes; of the 25 k most
473 connected transcripts, females had 76% transcripts assigning to a module, and males only 28%.
474 Importantly, this observation coincides with higher inter-individual variation in gene expression in
475 females than in males (Figure 1) and higher inter-individual variation in six phenotypes in females than in
476 males (Figure S5). When inter-individual variation in gene expression is low, transcripts will not be as
477 well clustered, because without variance there can be no co-variance for clustering algorithms to act upon
478 (Tritchler *et al.* 2009). Therefore, the lower variance in male gene expression may have resulted in the
479 observed lower module assignment. The observation of lower variation in phenotypes is an interesting
480 result that highlights similarities between transcriptomic and phenotypic expression. Building networks in
481 both sexes allowed for the identification of this lower assignment to modules in males, which may have
482 not been noted otherwise, as female modules generally were scored as preserved in males. Furthermore,
483 this allowed the identification of many male network modules with seemingly important and different
484 functional associations that in the female network were all grouped together into one very large module
485 (i.e., *darkred*). It will be valuable to inspect sex-specific module generation in other salmonids and in
486 tissues other than liver to understand the generality of these sex differences and associations to inter-
487 individual variance in gene expression and phenotypes.
488 Our observations confirm previous findings that co-expression patterns are often preserved
489 between sexes or closely related species (van Nas *et al.* 2009; Wong *et al.* 2014; Cheviron and Swanson

490 2017). Here, highly preserved modules between the sexes were often comprised of genes within pathways
491 involved in conserved functions. The most preserved modules between the sexes and species were
492 involved in basic cellular processes and included many co-expressed subunits of a multiple subunit
493 protein complex, such as translation machinery. Multiple subunits and closely related genes have long
494 been known to cluster together by co-expression (Eisen *et al.* 1998). Immunity-related modules were also
495 preserved between the sexes, with co-expression patterns similar to those observed previously in
496 salmonids (Sutherland, Koczka, *et al.* 2014). Considering the importance of immune function to both
497 sexes, it is not surprising that immunity modules are preserved between sexes.

498 The male-specific module *darkgrey* and the lowly preserved *green* were both associated with
499 size, which can be sexually dimorphic in salmonids and is associated to breeding success in males
500 (Blanchfield *et al.* 2003). There were no associations of female modules to length and weight (although
501 there was association to growth rate), which further emphasizes the potential for these male-specific
502 modules to be contributing to sexual dimorphism. The other male-specific module, *ivory*, may contribute
503 to sexual dimorphism and resolution of sexual antagonism by being an upstream controller of different
504 programs, as it is enriched for transcription factor activity and hub genes as putative transcription factors.
505 Hub genes of *ivory* include genes from the *wnt* protein family. Wnt signaling is associated with gonad
506 differentiation and shows sex-specific expression in several studies in mammals and fish (Vainio *et al.*
507 1999; Nicol and Guiguen 2011; Sreenivasan *et al.* 2014; Böhne *et al.* 2014). Future studies could
508 investigate whether transcription factors from the sex-specific *ivory* module control expression of
509 transcripts found to be sex-biased here once transcription factor binding sites are characterized in this
510 species.

511 The presence of sex-specific modules and sexually dimorphic gene expression in the liver
512 corresponds with what is known about sex hormones produced in the gonads, as these hormones have
513 been shown to regulate a significant proportion of the liver transcriptome in mouse (van Nas *et al.* 2009).
514 In a large-scale transcriptome study in humans, the liver was not one of the most sexually dimorphic in
515 terms of sex-biased genes (Chen *et al.* 2016). In oviparous species at a reproductive stage however, this
516 tissue is highly sexually dimorphic, given the role in females for producing oocyte constituents (e.g.
517 *vitellogenins*, *zona pellucida* proteins) (Qiao *et al.* 2016). Some of the strongest phenotypic associations
518 of female modules were to maturity. These associations may reflect the effects of sex hormones such as
519 estradiol, which controls reproduction and has a strong influence on transcription in fish (Garcia-Reyero
520 *et al.* 2018). There were no male modules associated to maturity, but there were only six females and two
521 males retained in the analysis that were immature, which prevents a comparison of maturation-related
522 transcripts between the sexes.

523 The ranking of module preservation levels in both the opposite sex and in Arctic Charr was often
524 similar, suggesting evolutionary conservation for many gene co-expression modules. Even with the lower
525 sample size in Arctic Charr, moderate and high preservation was identified for eight and three of the
526 female modules (n = 14), respectively, and for seven and 14 of the male modules (n = 25), respectively.
527 Modules preserved across species with significant phenotypic correlations may be worthwhile to
528 investigate further for future studies regarding their contribution to phenotypes such as growth rate,
529 reproduction, stress response, and immunity. For example, the preserved module in the male network,
530 *turquoise*, was enriched for immunity and marginally associated with growth (p = 0.05), phenotypes
531 known to trade-off (Lochmiller and Deerenberg 2000; van der Most *et al.* 2010).
532 Many sex-biased transcripts were identified (n = 6,983 transcripts) in comparison to only 154
533 transcripts found in sex-specific modules identified through the network comparison approach. Sex-
534 biased expression and sex-specific networks are not always overlapping phenomena (Chen *et al.* 2016).
535 This highlights large differences between these approaches, but in general they together provided a more
536 comprehensive result than either in isolation. The sex bias analysis found that neither male-biased nor
537 female biased genes were significantly overrepresented on the sex chromosome, but power to detect this
538 may have been reduced by the use of a reference genome of a related species rather than the target
539 species. In other species, male-biased transcripts are more often associated with migration to the sex
540 chromosome (Rowe *et al.* 2018), and although there was a trend towards this for the highly male-biased
541 transcripts here, it was not significant. The relationship of sex chromosomes, sex-biased gene expression
542 and sexual dimorphism is not yet well established (Dean and Mank 2014), and this study is an example of
543 integrating these multiple aspects for improved understanding of the role of transcriptomics in generating
544 sex differences.
545
546 *Case study: modules separated by immune response type*
547 Separate modules were identified for immune functions involving innate antiviral genes (i.e., male
548 *darkmagenta*) and innate immunity C-type lectins (i.e., male *steelblue*). This is of large interest
549 considering that these types of immune responses have been observed as responding inversely to different
550 agents, with pathogen recognition receptors (e.g. C-type lectins) potentially involved in ectoparasite
551 defense (Sutherland, Koczka, *et al.* 2014) and being up-regulated during out-migration of steelhead trout
552 *Oncorhynchus mykiss* smolts (Sutherland, Hanson, *et al.* 2014). In both of these observations, innate
553 antiviral genes were suppressed. Alternately, antiviral genes were overexpressed in non-migrating fish of
554 the same species, and were down-regulated in Pink Salmon *O. gorbuscha* infected with salmon lice
555 relative to controls (Sutherland, Koczka, *et al.* 2014). Even if the genes are not the same between these
556 studies and ours (i.e., no 1:1 association of orthologs has been done for these datasets), the observation of

557 similar functions in separate, but related, modules in the present study may indicate that these functions
558 are hardwired into different modules given that no known infection is occurring within these samples. It is
559 important to note that here unsigned networks were used, and therefore if the two immune response types
560 were completely inversely regulated, they would belong to the same module, which was not observed
561 here. These two modules may therefore not be completely under the same regulatory control as they are
562 not completely inversely correlated. This is a new observation in the regulation of these different immune
563 system processes in salmonids. This is an important avenue for further study given the relevance of these
564 genes to immune responses against pathogens, and the potential response outcomes of co-infection
565 occurring between parasitic and viral agents in nature.
566 The immune response modules observed here (i.e., male *darkmagenta*, *steelblue*, and *turquoise*)
567 were all considered as highly preserved between the sexes and moderately to highly conserved in Arctic
568 Charr. It will be valuable to see if these three modules or the genes found within them have conserved
569 expression patterns in other species as these may have important roles in defense responses. The tissue
570 was in a post-stress state, which could affect the induction of immune responses, and so additional
571 observations will be valuable. It is possible that the co-expression viewed in these (and other) modules
572 comes from the occurrence of a specific cell type that is present in different levels in the sampled tissue in
573 different individuals. Single-cell RNA-sequencing of immune cells, or *in situ* gene expression
574 hybridization techniques could address some of these questions. Further, to better understand the
575 immunity related modules, it may also be valuable to use a microbe profiling platform alongside
576 transcriptome studies of wild sampled individuals to best understand co-infection details (e.g. Miller *et al.*
577 2016). Nonetheless, the characterization of salmonid co-expression modules will be strengthened when
578 additional analyses are conducted with a broader range of species, once orthologs are identified among
579 the species.
580
581 *Future comparative approaches and salmonid transcriptome network evolution*
582 When similar datasets are produced in other salmonids, it will be valuable to identify whether the
583 preserved modules are conserved outside of the genus *Salvelinus*. However, importantly this will require
584 identification of 1:1 orthologs among the species, which would enable cross-species analyses. Salmonid
585 ortholog identification across reference transcriptomes has recently been conducted for Atlantic Salmon,
586 Brown Trout *Salmo trutta*, Arctic Charr, and European Whitefish *Coregonus lavaretus* (Carruthers *et al.*
587 2018), as well as Northern Pike (*Esox lucius*), Chinook Salmon (*O. tshawytscha*), Coho Salmon (*O.*
588 *kisutch*), Rainbow Trout (*O. mykiss*), Atlantic Salmon, and Arctic Charr (Christensen *et al.* 2018). This
589 type of approach, combined with non-redundant reference transcriptomes will be invaluable in future
590 studies to enable cross species comparisons.

If modules are indeed largely conserved between species, as our study suggests within *Salvelinus* liver, this would indicate that large-scale rewiring of baseline transcription networks has not occurred since the base of the lineage. The cases where species-specific modules are found will be highly valuable to investigate regarding the transcriptional architecture potentially underlying phenotypic differences between the species. The largest amount of rediploidization is thought to have occurred in the salmonids at the base of the lineage (Kodama *et al.* 2014; Lien *et al.* 2016), although a substantial proportion of ohnologs experienced lineage-specific rediploidization post-speciation events later in evolutionary time (Robertson *et al.* 2017). Given the large potential impact that divergence in regulatory regions or epigenetic signatures can have on gene expression, one could expect large lineage-specific changes in co-expression networks. The impact of the genome duplication and rediploidization on transcriptome networks, including lineage specific changes are important avenues for future study.

CONCLUSIONS

Co-expression networks and sex-biased expression of female and male Brook Charr liver in a reproductive season shortly after an acute handling stressor were characterized in the present study. Results support previous observations of moderate to high preservation of modules between sexes and closely related species. Highly preserved modules were involved in basic cellular functions and immune functions. Sex-specific modules identified only in the male network were enriched for transcription factor activities and associated with sex-biased or potentially sexually antagonistic phenotypes, such as body size. Higher assignment of transcripts to modules was identified in the female network, potentially due to higher inter-individual variance in gene expression and phenotypes. Important physiological functions such as immunity response types were captured by this analysis, identifying not only inverse regulation between two immunity responses but potentially decoupled regulation, which has implications for responses to co-infections and requires further study. This dataset has provided new insights into the transcriptome network structure differences between sexes and has pointed towards individual genes and gene modules that may be involved with generating sexually dimorphic phenotypes and potentially alleviating sexually antagonistic selection.

DATA ACCESSIBILITY

Brook Charr Phylofish transcriptome assembly (Pasquier *et al.* 2016):
http://phylofish.sigenae.org/ngspipelines/#!/NGSpipelines/Salvelinus%20fontinalis

Atlantic Salmon genome assembly (Lien *et al.* 2016):
https://www.ncbi.nlm.nih.gov/assembly/GCF_000233375.1

Complete and documented bioinformatics and analysis pipeline:
https://github.com/bensutherland/sfon_wgcna

SUPPLEMENTAL INFORMATION

Supplemental Results. Additional results including figures and tables that support the main text.

Additional File S1. All enrichment analyses for Gene Ontology biological process and molecular function categories. Includes all enrichment results with five or more genes in the category and with an enrichment $p \leq 0.01$ (no multiple test correction), and Swissprot identifiers within the category.

Additional File S2. Overview table for female and male modules, including module size, trait association, GO enrichment, preservation Zsummary and medianRank, and cross-tabulation results.

Additional File S3. Differential expression results for the sex-bias analysis, including $\log_2$ fold change values, p-values, identifiers and gene descriptions when available.

Additional File S4. Transcripts and module assignment in the female network along with Gene Significance and Module Membership values.

Additional File S5. Transcripts and module assignment in the male network along with Gene Significance and Module Membership values.

Additional File S6. Estimated counts file from eXpress used as input for network and differential expression analyses before low expression filtering and normalization.

ACKNOWLEDGEMENTS

Thanks to Guillaume Côté for laboratory assistance, Jérémy Le Luyer and Marie Filteau for discussions about WGCNA, Eric Normandeau for discussion on gene annotation, Yann Guiguen for discussion on details of transcriptome assembly, and Aimee-Lee Houde, three anonymous reviewers and the Editor for comments on the manuscript. This work was funded by a Fonds de Recherche du Québec (FRQ) Nature et Technologies research grant awarded to Céline Audet, Louis Bernatchez, and Nadia Aubin-Horth; a grant from the Société de Recherche et de Développement en Aquaculture Continentale (SORDAC) awarded to L.B. and C.A. J.M.P. is supported by the Finnish Cultural Foundation. During this work, B.J.G.S. was supported first by a Natural Sciences and Engineering Research Council of Canada postdoctoral fellowship and subsequently by an FRQ Santé postdoctoral fellowship.

654 # REFERENCES

655 Allendorf, F. W., and G. H. Thorgaard, 1984 Tetraploidy and the evolution of salmonid fishes, pp. 1–53
656 in *Evolutionary genetics of fishes*, edited by B. J. Turner. Plenum Publishing Corporation, New York.

657 Barson, N. J., T. Aykanat, K. Hindar, M. Baranski, G. H. Bolstad *et al.*, 2015 Sex-dependent dominance
658 at a single locus maintains variation in age at maturity in salmon. Nature 528: 405–408.

659 Blackmon, H., and Y. Brandvain, 2017 Long-term fragility of Y chromosomes is dominated by short-
660 term resolution of sexual antagonism. Genetics genetics.300382.2017–9.

661 Blanchfield, P. J., M. S. Ridgway, and C. C. Wilson, 2003 Breeding success of male brook trout
662 (*Salvelinus fontinalis*) in the wild. Mol. Ecol. 12: 2417–2428.

663 Bolger, A. M., M. Lohse, and B. Usadel, 2014 Trimmomatic: a flexible trimmer for Illumina sequence
664 data. Bioinformatics 30: 2114–2120.

665 Boula, D., V. Castric, L. Bernatchez, and C. Audet, 2002 Physiological, endocrine, and genetic bases of
666 anadromy in the Brook Charr, *Salvelinus fontinalis*, of the Laval River (Québec, Canada). Environ
667 Biol Fish 22: 229–242.

668 Böhne, A., T. Sengstag, and W. Salzburger, 2014 Comparative transcriptomics in East African Cichlids
669 reveals sex- and species-specific expression and new candidates for sex differentiation in fishes.
670 Genome Biology and Evolution 6: 2567–2585.

671 Bryant, D. M., K. Johnson, T. DiTommaso, T. Tickle, M. B. Couger *et al.*, 2017 A tissue-mapped Axolotl
672 *de novo* transcriptome enables identification of limb regeneration factors. Cell Reports 18: 762–776.

673 Bush, W. S., and J. H. Moore, 2012 Chapter 11: Genome-Wide Association Studies. PLoS Comput Biol
674 8: e1002822.

675 Carruthers, M., A. A. Yurchenko, J. J. Augley, C. E. Adams, P. Herzyk *et al.*, 2018 *De novo*
676 transcriptome assembly, annotation and comparison of four ecological and evolutionary model
677 salmonid fish species. BMC Genomics 19: 32.

678 Chen, C.-Y., C. M. Lopes-Ramos, M. L. Kuijjer, J. N. Paulson, A. R. Sonawane *et al.*, 2016 Sexual
679 dimorphism in gene expression and regulatory networks across human tissues. bioRxiv 1–34.

680 Cheviron, Z. A., and D. L. Swanson, 2017 Comparative transcriptomics of seasonal phenotypic flexibility
681 in two North American songbirds. Integr. Comp. Biol. 57: 1040–1054.

682 Christensen K. A., Rondeau E. B., Minkley D. R., Leong J. S., Nugent C. M., Danzmann R. G., Ferguson
683 M. M., Stadnik A., Devlin R. H., Muzzerall R., Edwards M., Davidson W. S., Koop B. F., 2018 The
684 Arctic charr (*Salvelinus alpinus*) genome and transcriptome assembly. PLoS ONE **13**: e0204076–30.

685 Crête-Lafrenière, A., L. K. Weir, and L. Bernatchez, 2012 Framing the Salmonidae family phylogenetic
686 portrait: a more complete picture from increased taxon sampling. PLoS ONE 7: e46662.

687 Dean, R., and J. E. Mank, 2014 The role of sex chromosomes in sexual dimorphism: discordance between
688 molecular and phenotypic data. Journal of Evolutionary Biology 27: 1443–1453.

689 Eisen, M. B., P. T. Spellman, P. O. Brown, and D. Botstein, 1998 Cluster analysis and display of genome-

690 wide expression patterns. Proceedings of the National Academy of Sciences 95: 14863–14868.

691 Ellegren, H., and J. Parsch, 2007 The evolution of sex-biased genes and sex-biased gene expression. Nat
692 Rev Genet 8: 689–698.

693 Filteau, M., S. A. Pavey, J. St-Cyr, and L. Bernatchez, 2013 Gene coexpression networks reveal key
694 drivers of phenotypic divergence in Lake Whitefish. Molecular Biology and Evolution 30: 1384–
695 1396.

696 Fleming, I. A., 1998 Pattern and variability in the breeding system of Atlantic salmon (*Salmo salar*), with
697 comparisons to other salmonids. Can. J. Fish. Aquat. Sci. 55: 59–76.

698 Gaiteri, C., Y. Ding, B. French, G. C. Tseng, and E. Sibille, 2014 Beyond modules and hubs: the potential
699 of gene coexpression networks for investigating molecular mechanisms of complex brain disorders.
700 Genes Brain Behav. 13: 13–24.

701 Garcia-Reyero, N., B. S. Jayasinghe, K. J. Kroll, T. Sabo-Attwood, and N. D. Denslow, 2018 Estrogen
702 signaling through both membrane and nuclear receptors in the liver of Fathead Minnow. General and
703 Comparative Endocrinology 257: 50–66.

704 Gillis, J., and P. Pavlidis, 2012 "Guilt by association" is the exception rather than the rule in gene
705 networks. PLoS Comput Biol 8: e1002444.

706 Horreo, J. L., 2017 Revisiting the mitogenomic phylogeny of Salmoninae: new insights thanks to recent
707 sequencing advances. PeerJ 5: e3828–10.

708 Huang, D. W., B. T. Sherman, and R. A. Lempicki, 2009 Systematic and integrative analysis of large
709 gene lists using DAVID bioinformatics resources. Nat Protoc 4: 44–57.

710 Kodama, M., M. S. O. Brieuc, R. H. Devlin, J. J. Hard, and K. A. Naish, 2014 Comparative mapping
711 between Coho Salmon (*Oncorhynchus kisutch*) and three other salmonids suggests a role for
712 chromosomal rearrangements in the retention of duplicated regions following a whole genome
713 duplication event. G3 - Genes|Genomes|Genetics 4: 1717–1730.

714 Langfelder, P., and S. Horvath, 2012 Fast R functions for robust correlations and hierarchical clustering.
715 J. Stat. Soft. 46: 1–17.

716 Langfelder, P., and S. Horvath, 2008 WGCNA: an R package for weighted correlation network analysis.
717 BMC Bioinformatics 9: 559.

718 Langfelder, P., R. Luo, M. C. Oldham, and S. Horvath, 2011 Is my network module preserved and
719 reproducible? PLoS Comput Biol 7: e1001057.

720 Langmead, B., and S. L. Salzberg, 2012 Fast gapped-read alignment with Bowtie 2. Nat Meth 9: 357–
721 359.

722 Li, H., B. Handsaker, A. Wysoker, T. Fennell, J. Ruan *et al.*, 2009 The Sequence Alignment/Map format
723 and SAMtools. Bioinformatics 25: 2078–2079.

724 Lien, S., B. F. Koop, S. R. Sandve, J. R. Miller, M. P. Kent *et al.*, 2016 The Atlantic Salmon genome
725 provides insights into rediploidization. Nature 533: 200–205.

726 Lochmiller, R. L., and C. Deerenberg, 2000 Trade-offs in evolutionary immunology: just what is the cost
727 of immunity? Oikos 88: 87–98.

728 Mackay T. F., 2001 The genetic architecture of quantitative traits. Annu. Rev. Genet. 35: 303–339.

729 Mackay T. F. C., Stone E. A., Ayroles J. F., 2009 The genetics of quantitative traits: challenges and
730 prospects. Nat Rev Genet 10: 565–577.

731 MacManes, M. D., 2014 On the optimal trimming of high-throughput mRNA sequence data. Front.
732 Genet. 5: 13.

733 Macqueen, D. J., and I. A. Johnston, 2014 A well-constrained estimate for the timing of the salmonid
734 whole genome duplication reveals major decoupling from species diversification. Proceedings of the
735 Royal Society B: Biological Sciences 281: 20132881–20132881.

736 Mähler, N., J. Wang, B. K. Terebieniec, P. K. Ingvarsson, N. R. Street *et al.*, 2017 Gene co-expression
737 network connectivity is an important determinant of selective constraint. PLoS Genet 13: e1006402.

738 Miller, K. M., I. A. Gardner, R. Vanderstichel, T. Burnley, S. Li *et al.*, 2016 Report on the performance
739 evaluation of the Fluidigm BioMark platform for high-throughput microbe monitoring in salmon:, 1–
740 293 p.

741 Mueller, A. J., E. G. Canty-Laird, P. D. Clegg, and S. R. Tew, 2017 Cross-species gene modules emerge
742 from a systems biology approach to osteoarthritis. NPJ Syst Biol Appl 3: 13.

743 Nicol, B., and Y. Guiguen, 2011 Expression profiling of wnt signaling genes during gonadal
744 differentiation and gametogenesis in Rainbow Trout. Sex Dev 5: 318–329.

745 Oldham, M. C., S. Horvath, and D. H. Geschwind, 2006 Conservation and evolution of gene coexpression
746 networks in human and chimpanzee brains. Proceedings of the National Academy of Sciences 103:
747 17973–17978.

748 Parsch, J., and H. Ellegren, 2013 The evolutionary causes and consequences of sex-biased gene
749 expression. Nature Publishing Group 14: 83–87.

750 Pasquier, J., C. Cabau, T. Nguyen, E. Jouanno, D. Severac *et al.*, 2016 Gene evolution and gene
751 expression after whole genome duplication in fish: the PhyloFish database. BMC Genomics 17: 368.

752 Poley, J. D., B. J. G. Sutherland, S. R. M. Jones, B. F. Koop, and M. D. Fast, 2016 Sex-biased gene
753 expression and sequence conservation in Atlantic and Pacific salmon lice (Lepeophtheirus salmonis).
754 BMC Genomics 17: 483.

755 Prokkola, J. M., M. Nikinmaa, M. Lewis, K. Anttila, M. Kanerva *et al.*, 2018 Cold temperature represses
756 daily rhythms in the liver transcriptome of a stenothermal teleost under decreasing day length. J. Exp.
757 Biol. 221: jeb170670.

758 Qiao, Q., S. Le Manach, B. Sotton, H. Huet, E. Duvernois-Berthet *et al.*, 2016 Deep sexual dimorphism in
759 adult medaka fish liver highlighted by multi-omic approach. Sci. Rep. 6: 32459.

760 Quinlan, A. R., and I. M. Hall, 2010 BEDTools: a flexible suite of utilities for comparing genomic
761 features. Bioinformatics 26: 841–842.

Quinn, T. P., and C. J. Foote, 1994 The effects of body size and sexual dimorphism on the reproductive behavior of sockeye salmon, *Oncorhynchus nerka*. Animal Behaviour 48: 751–761.

R Core Team, 2018 R: A language and environment for statistical computing. R Foundation for Statistical Computing.

Roberts, A., and L. Pachter, 2013 Streaming fragment assignment for real-time analysis of sequencing experiments. Nat Meth 10: 71–73.

Robertson, F. M., M. K. Gundappa, F. Grammes, T. R. Hvidsten, A. K. Redmond *et al.*, 2017 Lineage-specific rediploidization is a mechanism to explain time-lags between genome duplication and evolutionary diversification. Genome Biol. 18: 111.

Robinson, M. D., and A. Oshlack, 2010 A scaling normalization method for differential expression analysis of RNA-seq data. Genome Biol. 11: R25.

Robinson, M. D., D. J. McCarthy, and G. K. Smyth, 2010 edgeR: a Bioconductor package for differential expression analysis of digital gene expression data. Bioinformatics 26: 139–140.

Rose, N. H., F. O. Seneca, and S. R. Palumbi, 2015 Gene networks in the wild: identifying transcriptional modules that mediate coral resistance to experimental heat stress. Genome Biology and Evolution 8: 243–252.

Rowe, L., S. F. Chenoweth, and A. F. Agrawal, 2018 The Genomics of Sexual Conflict. The American Naturalist 192: 274–286.

Sauvage, C., M. Vagner, N. Derôme, C. Audet, and L. Bernatchez, 2012a Coding gene single nucleotide polymorphism mapping and quantitative trait loci detection for physiological reproductive traits in Brook Charr, *Salvelinus fontinalis*. G3 - Genes|Genomes|Genetics 2: 379–392.

Sauvage, C., M. Vagner, N. Derôme, C. Audet, and L. Bernatchez, 2012b Coding gene SNP mapping reveals QTL linked to growth and stress response in Brook Charr (*Salvelinus fontinalis*). G3 - Genes|Genomes|Genetics 2: 707–720.

Sreenivasan, R., J. Jiang, X. Wang, R. Bártfai, H. Y. Kwan *et al.*, 2014 Gonad differentiation in Zebrafish is regulated by the canonical wnt signaling pathway. Biology of Reproduction 90: e34397–10.

Sutherland, B. J. G., T. Gosselin, E. Normandeau, M. Lamothe, N. Isabel *et al.*, 2016 Salmonid chromosome evolution as revealed by a novel method for comparing RADseq linkage maps. Genome Biology and Evolution 8: 3600–3617.

Sutherland, B. J. G., K. C. Hanson, J. R. Jantzen, B. F. Koop, and C. T. Smith, 2014 Divergent immunity and energetic programs in the gills of migratory and resident Oncorhynchus mykiss. Mol. Ecol. 23: 1952–1964.

Sutherland, B. J. G., K. W. Koczka, M. Yasuike, S. G. Jantzen, R. Yazawa *et al.*, 2014 Comparative transcriptomics of Atlantic *Salmo salar*, Chum *Oncorhynchus keta* and Pink Salmon *O. gorbuscha* during infections with salmon lice *Lepeophtheirus salmonis*. BMC Genomics 15: 200.

Sutherland, B. J. G., C. Rico, C. Audet, and L. Bernatchez, 2017 Sex chromosome evolution, heterochiasmy, and physiological QTL in the salmonid Brook Charr *Salvelinus fontinalis*. G3 -

Genes|Genomes|Genetics 7: 2749–2762.

Thompson, D., A. Regev, and S. Roy, 2015 Comparative analysis of gene regulatory networks: from network reconstruction to evolution. Annu. Rev. Cell Dev. Biol. 31: 399–428.

Tritchler, D., E. Parkhomenko, and J. Beyene, 2009 Filtering Genes for Cluster and Network Analysis. BMC Bioinformatics 10: 193–9.

Vainio, S., M. Heikkilä, A. Kispert, N. Chin, and A. P. McMahon, 1999 Female development in mammals is regulated by Wnt-4 signalling. Nature 397: 405–409.

van Dam, S., U. Võsa, A. van der Graaf, L. Franke, and J. P. de Magalhães, 2017 Gene co-expression analysis for functional classification and gene-disease predictions. Brief Bioinform.

van der Most, P. J., B. de Jong, H. K. Parmentier, and S. Verhulst, 2010 Trade-off between growth and immune function: a meta-analysis of selection experiments. Functional Ecology 25: 74–80.

van Nas, A., D. Guhathakurta, S. S. Wang, N. Yehya, S. Horvath *et al.*, 2009 Elucidating the role of gonadal hormones in sexually dimorphic gene coexpression networks. Endocrinology 150: 1235–1249.

Warnes, G. R., B. Bolker, L. Bonebakker, R. Gentleman, W. Hubert *et al.*, 2016 gplots: Various R Programming Tools for Plotting Data.

Wijchers, P. J., and R. J. Festenstein, 2011 Epigenetic regulation of autosomal gene expression by sex chromosomes. Trends Genet. 27: 132–140.

Wong, R. Y., M. M. McLeod, and J. Godwin, 2014 Limited sex-biased neural gene expression patterns across strains in Zebrafish (Danio rerio). BMC Genomics 15: 905–10.

Wright, A. E., M. Fumagalli, C. R. Cooney, N. I. Bloch, F. G. Vieira *et al.*, 2018 Male-biased gene expression resolves sexual conflict through the evolution of sex-specific genetic architecture. Evolution Letters 2: 52–61.

Wu, T. D., and C. K. Watanabe, 2005 GMAP: a genomic mapping and alignment program for mRNA and EST sequences. Bioinformatics 21: 1859–1875.

825 # TABLES AND FIGURES

826 **Table 1.** Female modules shown with the number of transcripts within the module (n), the general
827 category of traits correlated with the module ($p \leq 0.01$), the most significantly enriched Gene Ontology
828 category (Biological Process), the Zsummary for preservation of the module in Brook Charr males (BC
829 m) and Arctic Charr males (AC m), as well as the module quality (robustness). Zsummary < 2 is not
830 preserved, 2 < Zsummary < 10 is moderately preserved, and > 10 is preserved. The *grey* module includes
831 unassigned genes and the *gold* module is a random selection of 1000 genes from the assigned modules for
832 testing preservation metrics. Full module-trait correlations are shown in Figure 2, full GO enrichment in
833 Additional File S1, and expanded summaries of this table in Additional File S2.
834

Module	n	Traits	GO Enrichment (BP)	Preservation BC m | AC m		Quality
green	725	blood	translation	100	24	75
blue2	1762	blood; liver; maturity; RIN	ribonucleoprotein complex biogenesis	71	32	58.5
salmon	449	liver; maturity; RIN	erythrocyte development	56	17	42
darkorange	805	blood	small molecule metabolic process	48	8.8	36
lightsteelblue	77	blood	*none*	48	8.2	25.5
ivory	451	-	ER-associated ubiquitin-dependent protein catabolic process	37	5.4	25.5
thistle2	834	maturity	tissue development	29	3.6	36.5
indianred4	1180	blood; growth; liver; maturity; RIN	membrane assembly	28	2.8	22
coral1	689	liver; maturity; RIN	regulation of cell growth	25	5.2	34
thistle3	235	blood; liver; size	inorganic anion transmembrane transport	24	1.2	21
skyblue1	96	RIN	intracellular signal transduction	17	1.2	21
darkmagenta	1072	blood; maturity	single-organism metabolic process	13	5	58
coral2	200	-	regulation of blood circulation	11	2.8	14
grey	5892	Not a module	Not a module	9	2.4	-18
gold	1k*	blood; size	Not a module	4.8	0.38	-0.86
darkred	10533	blood	protein ubiquitination	4.5	-0.55	23.5

835

836

837 **Table 2.** Male modules with the number of transcripts within the module (n), the general category of
838 traits correlated with the module ($p \leq 0.01$), the most significantly enriched Gene Ontology category
839 (Biol. Proc.), the Zsummary for preservation of the module in Brook Charr females (BC f) and Arctic
840 Charr males (AC m), as well as the identified module quality (robustness). Zsummary < 2 is not
841 preserved, 2 < Zsummary < 10 is moderately preserved, and > 10 is preserved. The *grey* module includes
842 unassigned genes and the *gold* module is a random selection of 1000 genes from the assigned modules for
843 testing preservation metrics. Full module-trait correlations are shown in Figure S8, full GO enrichment in
844 Additional File 1, and expanded summaries of this table in Additional File S2.

Module	n	Traits	GO Enrichment (BP)	Preservation BC f | AC m		Quality
yellow	339	blood; liver; size	translation	58	24	51
tan	173	blood; size	*none*	43	18	41.5
brown	1732	blood; sperm	ribonucleoprotein complex biogenesis	38	39	72.5
lightcyan	734	blood; size	organic acid metabolic process	34	21	69
magenta	226	*none*	response to endoplasmic reticulum stress	32	38	45
darkmagenta	61	*none*	defense response to virus	27	16	25.5
darkgreen	724	blood; growth; liver; size	*none*	24	11	58
steelblue	65	blood; growth; sperm	positive regulation of innate immune response	22	6.2	26.5
violet	64	liver	sterol biosynthetic process	21	10	29.5
grey60	147	*none*	secretion by cell	20	11	39
lightsteelblue1	55	*none*	*none*	15	0.85	23
yellowgreen	61	blood	*none*	13	0.24	24.5
turquoise	783	*none*	immune system process	12	14	68.5
orangered4	57	sperm	regulation of apoptotic process	12	2.3	26.5
floralwhite	52	*none*	glutathione metabolic process	11	13	25
paleturquoise	64	blood	response to organonitrogen compound	10	7.8	25.5
lightcyan1	791	blood; sperm	cytokinesis	9.7	11	67.5
sienna3	61	liver; size	extracellular structure organization	9.6	14	26.5
plum1	58	*none*	*none*	9.6	7.4	23.5
mediumpurple3	57	size	ribonucleoprotein complex assembly	8.4	5.3	20.5
darkolivegreen	138	blood	*none*	7.6	11	28.5
skyblue	78	RIN	regulation of transcription, DNA-templated	6.7	5.8	28
grey	17992	*Not a module*	*Not a module*	5.5	2.3	-14
gold	1k*	*Not a module*	*Not a module*	4.9	3.2	-0.035
green	334	size	translation	4.5	3.1	39
darkgrey	100	size	small molecule metabolic process	1.8	-0.28	31.5
ivory	54	blood	neurogenesis	0.81	0.22	24

845

Table 3. Sex-biased transcript presence in modules that are either unique to each sex (low module preservation), or moderately or highly preserved, along with the number and percentage of the transcripts within each sex's sex-biased transcript category (e.g. female high sex-bias). These counts only include expressed transcripts that are assigned to modules in the network analysis for each sex.

Sex	Module Preservation in opposite sex	All expressed transcripts count	Moderate sex bias (1.5-4-fold)	High sex bias (>4-fold)
Female	Low	0 (0%)	0 (0%)	0 (0%)
	Medium	9,613 (54.8%)	744 (52.0%)	31 (53.4%)
	High	7,929 (45.2%)	687 (48.0%)	27 (46.6%)
Total	-	17,542	1,431	58
Male	Low	147 (2.3%)	19 (2.6%)	0 (0%)
	Medium	1,350 (21.1%)	119 (16.5%)	1 (2.7%)
	High	4,886 (76.5%)	584 (80.9%)	36 (97.3%)
Total		6,383	722	37

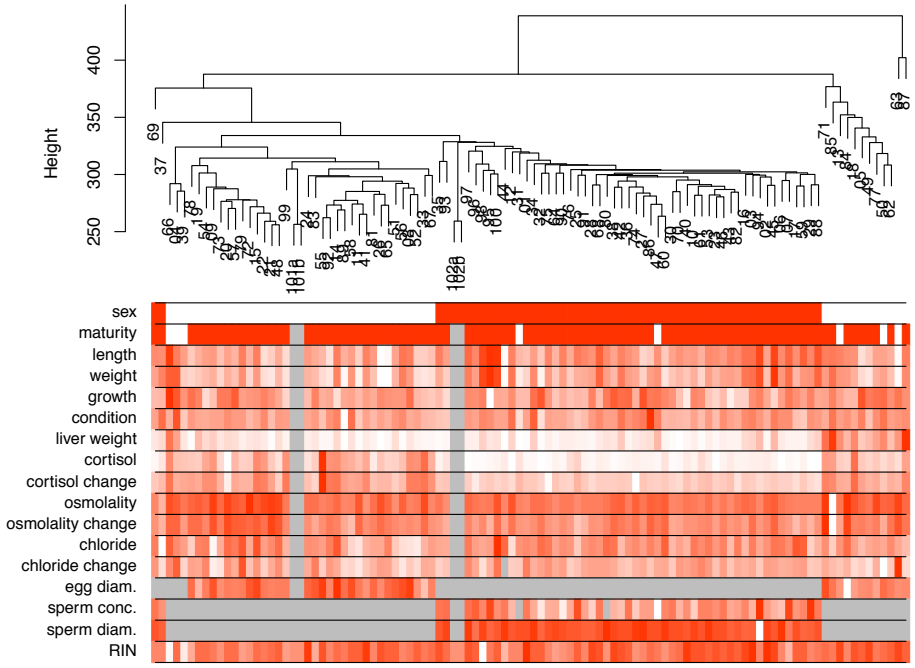

Figure 1. Brook Charr individual samples clustered by gene expression similarity in the liver using all genes with corresponding quantitative trait values shown in the heatmap below the dendrogram with intensity of red reflecting the normalized trait value for that sample. Sex was the largest factor affecting the data (see heatmap sex row; white = females; red = males). Parents were sequenced in duplicate, and clustered with the offspring of their respective sex (see 101ab for mother and 102ab for father; parents have grey missing data values for all phenotypes but sex and RIN). Females with large liver weight clustered outside the other female samples (see on the right-hand side on the liver weight row), and were removed as they were considered outliers (see Methods).

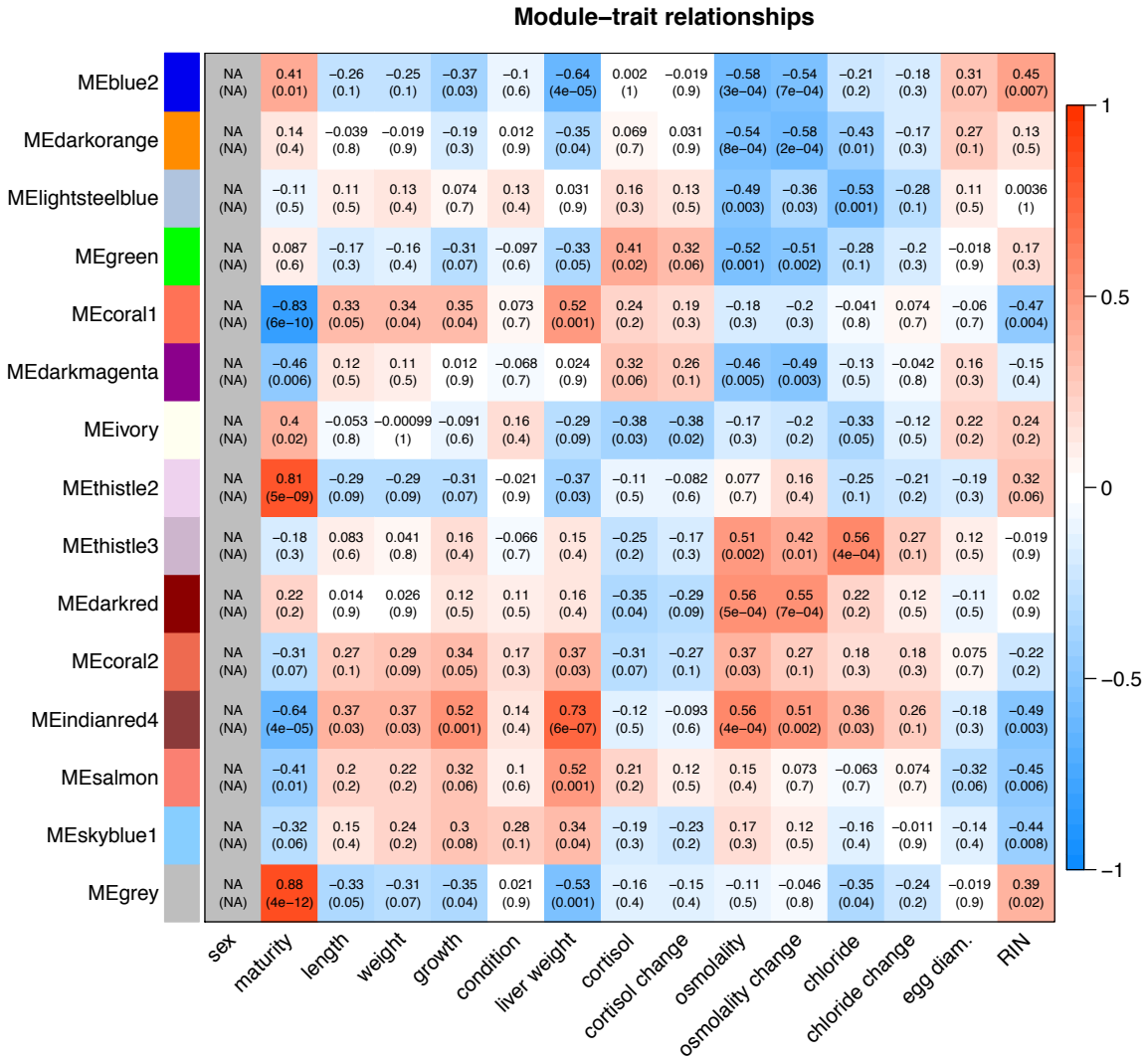

Figure 2. Module-trait relationships for Brook Charr females, including Pearson correlation r-value and p-values. The boldness of color indicates the strength of the relationship. Module-trait correlations are also shown in Table 1 with more general grouping of traits alongside other metrics such as module size and enriched Gene Ontology categories. The male network module-trait relationships are shown in Figure S8.

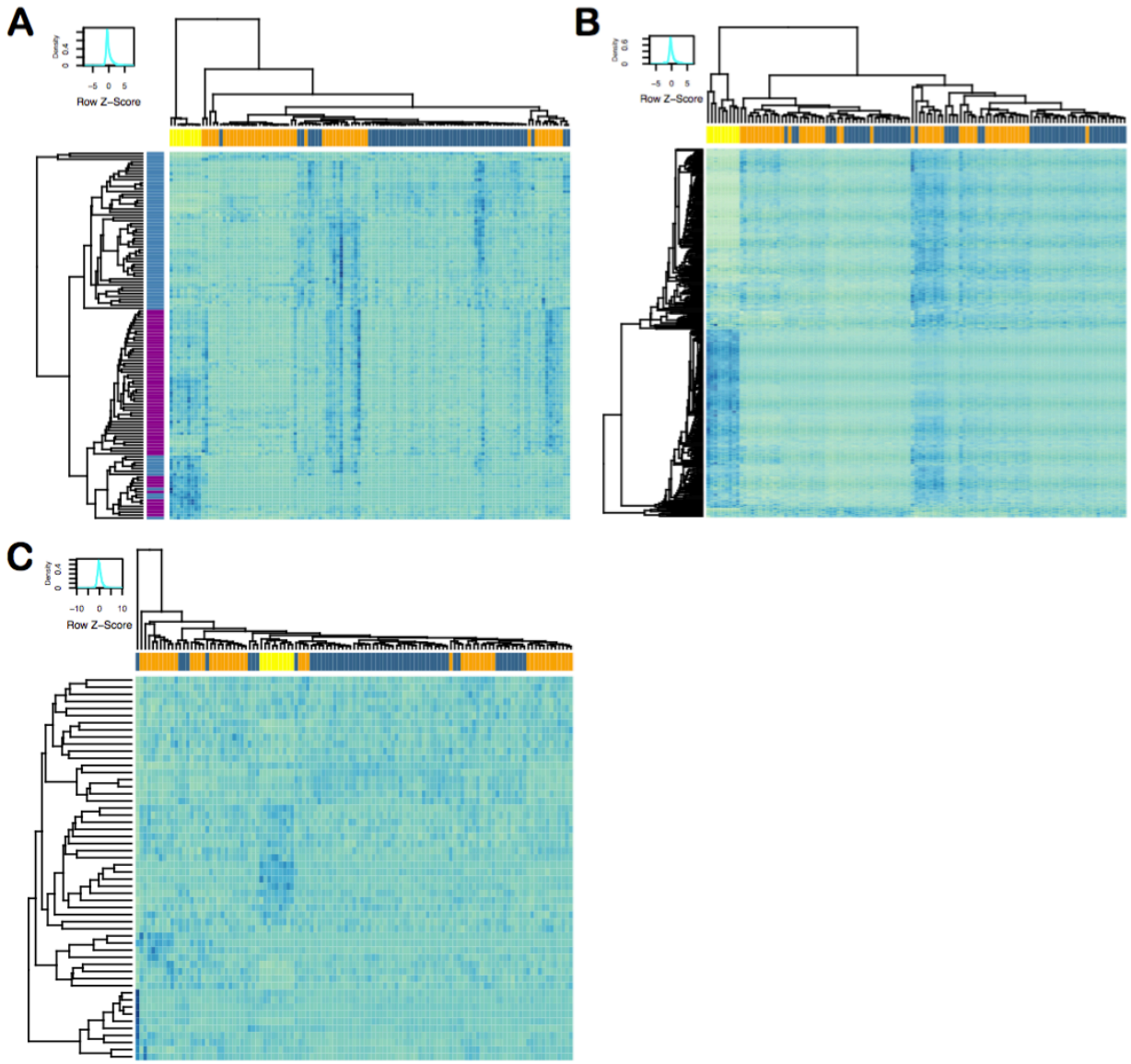

Figure 3. Heatmaps of expression of transcripts within (A) two immunity-related male modules, *steelblue* and *darkmagenta*, which are related to innate immunity and innate antiviral immunity, respectively, (B) the preserved male module *yellow* (translation), and (C) the male-specific *ivory* (transcription factor activity). Samples are shown on the horizontal with Brook Charr females (orange), Brook Charr males (blue), and Arctic Charr males (in yellow). Transcripts from multiple modules in (A) are coloured according to the module (steelblue, darkmagenta). The normalized expression values are shown within the heatmap.